Formation control of differential-drive robots with input saturation and constraint on formation size

Ayush Agrawal[1], Mukunda Bharatheesha[2] and Shishir Kolathaya[3]

***Abstract*— Cooperative control involves developing control strategies for individual robots that guarantee synchronized behavior of the states of all the robots in a team in some prescribed sense. In this work, we present a novel controller that achieves formation control for a group of differential-drive robots. First, we propose a nonlinear feedback control law that guarantees stable tracking of a reference trajectory for a single robot without exceeding the velocity limits of the robot. Using Lyapunov analysis, we obtain the necessary conditions on the control parameters and establish ultimate boundedness on error terms. Next, we formulate the formation control problem as a trajectory tracking problem for the multi-robot system and solve it using the proposed controller. Additionally, we provide constraints on formation size for given reference trajectory which ensures smooth turning of multi-robot formation without exceeding actuation limits.**

I. INTRODUCTION

Researchers, in modern times, recognize cooperative control as a potential solution to complex problems such as carrying heavy objects, search and rescue missions, and satellite clustering [11]. Formation control is considered a cooperative strategy for the positions and orientations of robots in a multi-robot system [4]. Formation control methods in literature are broadly categorized under leader-follower methods [1], [3], virtual structure methods [4], [5], graph theory methods [6], [8]-[12], behavior-based methods [13], and artificial potential field based methods [14].

The authors in [1] proposed a controller to achieve trajectory tracking and collision avoidance (CA) for a single robot, and for leader follower formation control. However, the proposed controller fails to obey the actuation limit of the robots, and the stability condition presented in [1] is weak and does not establish the boundedness on the error terms for time-varying trajectory. Unlike [1], where authors defined positions of followers using fixed distance and orientation relative to the leader, [2] uses curvilinear coordinates to determine the follower position relative to its assigned leader in the multi-vehicle system. Although this feature allows the formation to navigate flexibly on uneven terrains, the controller requires a finite segment of the leader's motion history to compute follower positions. A leader-follower formation control strategy with input saturation is given in [3]. The input constraints restrict the set of possible paths for the leader and the follower robots. The above methods are susceptible to single-point failure, i.e., the whole system will fail if communication with the leader is lost.

The virtual structure method solves this issue. The authors in [4] generate a virtual robot based on the formation structure and control its motion along the desired trajectory using backstepping and Lyapunov-based controller. The controller ensures collision avoidance but fails to keep the speeds below practical limits. A hybrid approach is proposed in [5], where a Lyapunov-based controller controls the position of the virtual leader, which is fed to a graph-theory-based position controller to control the offset between the followers. The control inputs are within the actuation limits; however, the convergence time is very large.

Instead of feeding the formation group trajectory to each robot, the pose information of neighboring robots is sufficient to achieve formation control. Researchers in [6], [8]-[12] have modeled the communication topology for a group of robots using the Laplacian matrix. In [6], the presence of root makes the system prone to single point failure. Like [1], [5], formation generated in [6] lacks rotational degree of freedom. A synchronous approach to formation control is given in [7], [8], where the defined tracking and synchronization errors were asymptotically driven to zero using Lyapunov-based controllers. In [7], synchronization error is specified for every pair of interacting agents, while in [8], it depends on the communication topology of the multi-robot system. The algorithm in [7] ensures practical input magnitudes, but unlike [8], [11], it does not account for the effects of communication delay.

In this paper, we present a novel controller that ensures stable tracking of a reference trajectory while keeping robot's velocity within practical limits. Then, we rigorously prove the stability of robot's tracking manoeuvre for time-varying trajectory. Later on, we use virtual structure method to address the formation control problem and solve it using the proposed controller. We also discuss the affects of large formation size on the kinematics of the robots for a given reference trajectory. The paper is organized as follows: In Section II, we design a controller that obeys input constraints and guarantees trajectory tracking. In Section III, we formulate the formation control problem as a trajectory tracking problem and discuss some constraints on the formation size for a given reference trajectory to avoid breach of velocity

[1] Ayush Agarwal has received his Bachelor's degree from the Department of Mechanical Engineering at the Indian Institute of Technology Bombay, India. ayush.agrawal.c2021@iitbombay.org, aayush.agrawal149@gmail.com

[2]Mukunda Bharatheesha is a guest faculty at Robert Bosch Centre for Cyber Physical Systems and a Senior Member of Techinal Staff at ARTPARK, Indian Institute of Science, Bengaluru, India mukundab@iisc.ac.in, mukunda@artpark.in

[3]Shishir Kolathaya is an Assistant Professor at Robert Bosch Centre for Cyber Physical Systems and the department of Computer Science and Automation (CSA), Indian Institute of Science, Bengaluru, India shishirk@iisc.ac.in

Manuscript 458 submitted to 2023 American Control Conference (ACC).
Received October 2, 2022.

limits in robots. In Section IV, we draw some conclusions and discuss some aspects of future work.

II. TRAJECTORY TRACKING CONTROLLER WITH INPUT CONSTRAINTS

We consider a differential-drive robot (see Fig.1) with wheels driven by identical motors. The radius of the wheel is R, and the distance between the center of the two wheels (track width) is L. The instantaneous angular speed of the left and right wheel are denoted by ω_l and ω_r respectively. The maximum limit on the angular speed of both the motors is $\omega_{r,\,l}^{max}$. In Fig.1, v denote the linear velocity of the center of axle, and ω denote the angular velocity of the robot about the axis passing through the center of axle (perpendicular to the plane of paper). We can express $v,\ \omega$ as a function of $\omega_l,\ \omega_r$ as follows

$$\begin{bmatrix} v \\ \omega \end{bmatrix} = \begin{bmatrix} R/2 & R/2 \\ R/L & -R/L \end{bmatrix} \begin{bmatrix} \omega_r \\ \omega_l \end{bmatrix} \tag{1}$$

The kinematics of the differential-drive robot is governed by the following set of ordinary differential equations

$$\begin{aligned} \dot{x} &= \tfrac{R(\omega_r+\omega_l)}{2}\cos(\theta) = v\cos(\theta) \\ \dot{y} &= \tfrac{R(\omega_r+\omega_l)}{2}\sin(\theta) = v\sin(\theta) \\ \dot{\theta} &= \tfrac{R(\omega_r-\omega_l)}{L} \qquad\quad = \omega \end{aligned} \tag{2}$$

where $[x,\ y]^T \in \mathbb{R}^2$ are the Cartesian coordinates, $\theta \in \mathbb{R}$ is the orientation of the robot with respect to the global x-axis (see Fig.1). The robot has to follow a reference trajectory given by $(x_d(t),\ y_d(t))$ where $t \geq 0$ denotes time. Let $v_{max},\ \omega_{max}$ denote the maximum permissible values of $v,\ \omega$ respectively. Selecting [1]

$$v_{max} = \frac{R\omega_{r,\,l}^{max}}{2}, \quad \omega_{max} = \frac{R\omega_{r,\,l}^{max}}{L} \tag{3}$$

will ensure that $\omega_r,\ \omega_l$ never exceed $\omega_{r,\,l}^{max}$. Note that $v_{max},\ \omega_{max}$ are dependent on $\omega_{r,\,l}^{max}$ but the two quantities have different magnitudes.

Note 1: The reference trajectory is defined as motion of a point whose coordinates at a particular time, $t \geq 0$, is given by $[x_d(t),\ y_d(t)]$. It is a time varying trajectory. In principle, the robot has to chase a point whose coordinates $(x_d(t),\ y_d(t))$ are continuous function of time, $t \geq 0$.

We define the position errors as, $e_x(t) = x(t) - x_d(t),\ e_y(t) = y(t) - y_d(t)$. For $(e_x,\ e_y) \neq (0,\ 0)$, we also define the desired orientation as $\theta_d = \arctan 2(e_y, e_x)$, and the orientation error as $e_\theta = \theta - \theta_d$ as shown in Fig. 2. It should be noted that θ_d gives the instantaneous desired direction of motion for the robot at a time $t \geq 0$, that depends on the current position of the robot, $(x(t),\ y(t))$, and the current point on the reference trajectory, $(x_d(t),\ y_d(t))$. The discontinuous nature of the function - $\arctan 2(\cdot,\ \cdot)$ can cause disruptions in the direction of motion of the robot. Hence for $(e_x,\ e_y) \neq (0,\ 0)$, we define the continuous form of θ_d using the *unwrap* function [16] as:

$$\theta_d = \arctan 2(e_y,\ e_x)\big|_{unwrap} \tag{4}$$

[1]Refer section III-A of [17] to see how $v_{max},\ \omega_{max}$ are selected as in (3).

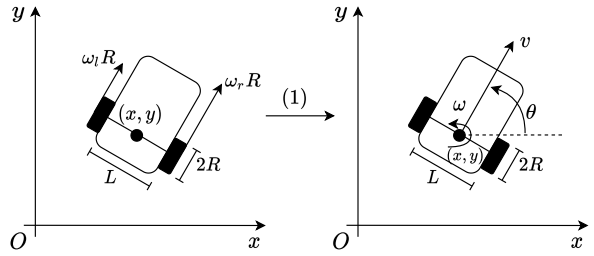

Fig. 1: Differential-drive kinematics: Transformation of control inputs from $[\omega_r,\ \omega_l]^T$ to $[v,\ \omega]^T$ using (1)

Some configuration might lead to singular direction, and impractically high magnitudes of linear and angular acceleration, see Fig.2. To avoid such cases, we assume throughout the paper that the reference trajectory has the following characteristics:

Assumption 1: The reference trajectory is smooth, i.e. both $x_d(t),\ y_d(t)$ are smooth function of time, $\forall\ t > 0$, and the first derivatives of $x_d(t),\ y_d(t)$, i.e., $\dot{x}_d(t),\ \dot{y}_d(t)$ are bounded. Moreover, the reference trajectory is such that it does not initiate sharp turns in robot with respect to the current orientation of the robot, i.e.,

$$\cos(e_\theta) \in [-1,\ -\delta_\theta] \cup [\delta_\theta,\ 1] \tag{5}$$

for some $\delta_\theta \in (0, 1)$.

Note 2: The value of δ_θ corresponding to a given initial pose of robot and a given reference trajectory is fixed and must lie in the interval $(0,\ 1)$.

Remark 1: Assumption 1 on the reference trajectory implies that scenarios shown in Fig.2 should be avoided.

1) In Fig.2(a), the robot cannot move along the desired direction of motion (singular direction, $e_\theta = \frac{\pi}{2}$) due to non-holonomic constraint.
2) In Fig.2(b), for the robot to keep following the reference trajectory on sharp turns at $t = t_2,\ t_3$, theoretically infinite angular acceleration (in motors) will be required.
3) The singularity condition $e_x = e_y = 0$ can be easily handled using zero controllers $v = \omega = 0$. It is very unlikely to experience this condition with real systems, hence we won't investigate this case further in our work.
4) The condition in (5) is not too restrictive since the robot can perform in-place rotation to reorient itself in case the condition is not met.

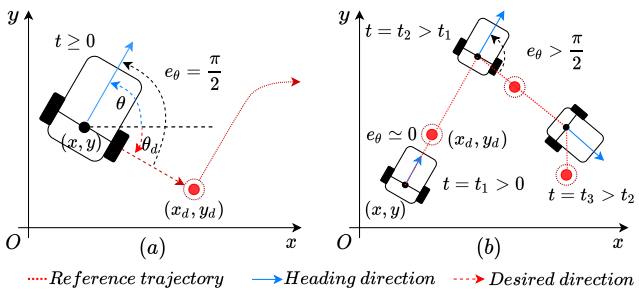

Fig. 2: (a) $e_\theta = \pi/2$, violation of non-holonomic constraint, (b) Sharp turn lead to sudden change in value of e_θ

Manuscript 458 submitted to 2023 American Control Conference (ACC).
Received October 2, 2022.

Assumption 2: Define $\hat{\dot{\theta}}_d$ to be an estimate of $\dot{\theta}_d$ where,

$$\dot{\theta}_d = \frac{e_x\dot{e}_y - e_y\dot{e}_x}{D^2}, \quad D = \sqrt{e_x^2 + e_y^2} \tag{6}$$

At every time instant, we compute $\theta_d(t)$ using (4). With the value of $\theta_d(t)$ at current and previous time step, and using backward difference method we can estimate $\hat{\dot{\theta}}_d$ as follows

$$\hat{\dot{\theta}}_d(t) = \frac{\theta_d(t) - \theta_d(t-\tau)}{\tau} \tag{7}$$

where $\tau \in (0,\ 1)$ represents simulation time step. The estimation error in $e_x(t),\ e_y(t)$ (estimated using odometry) will propogate while computing $\hat{\dot{\theta}}_d(t)$. Hence, there exists an estimation error in $\hat{\dot{\theta}}_d(t)$ relative to $\dot{\theta}_d$. We denote the error by a small positive number, ε_θ, as follows

$$|\hat{\dot{\theta}}_d - \dot{\theta}_d| \leq \varepsilon_\theta = \Omega(\tau)^2, \quad \varepsilon_\theta \in \mathbb{R}_{>0} \tag{8}$$

In a practical setting, the value of ε_θ depends on the sensor resolution, robot's specification, and the reference trajectory.

Assumption 3: The maximum translational speed of robot, v_{max} is much greater than $|v_{traj}^{sup}| = \sup_{t\geq 0} \sqrt{\dot{x}_d^2 + \dot{y}_d^2}$ such that

$$\frac{v_{max}\delta_\theta^2}{|v_{traj}^{sup}|} > 1 \tag{9}$$

for a given $\delta_\theta \in (0,\ 1)$.

Remark 2: Condition (9) is also not restrictive. Planning a reference trajectory such that $|v_{traj}^{sup}| < v_{max}$ will satisfy the practical requirement for the robot to be faster than the reference trajectory it should track.

The robot will approach the reference trajectory and stable tracking will be achieved if the error terms e_x, e_y, e_θ, converge to a neighbourhood close to the origin in finite time such that,

$$\left\|e_x, e_y\right\|_2 = D(t) \leq b_D, \quad |e_\theta(t)| \leq b_{e_\theta} \qquad \forall\ t \geq T \tag{10}$$

for some small positive number $b_D, b_{e_\theta} > 0$.

Theorem 1. *Consider a robot whose kinematics is defined as in (2) and has a maximum linear and angular speed as $v_{max}, \omega_{max} > 0$ respectively (3). The reference trajectory is described as $(x_d(t),\ y_d(t))$ that satisfies assumptions 1, 2 and 3. Then, stable tracking (10) is guaranteed without exceeding actuator limits if the following closed-loop feedback controller is applied,*

$$v = -v_{max}\cos(e_\theta)\frac{\eta_v D}{1+\eta_v D} \tag{11}$$

$$\omega = -(\omega_{max} - \Omega_{max})\tanh(\eta_\omega e_\theta) + \hat{\dot{\theta}}_d \tag{12}$$

for $D = \sqrt{e_x^2 + e_y^2}$ and positive constants $\eta_v,\ \eta_\omega,\ \Omega_{max} > 0$. The choice of Ω_{max}, η_v satisfy

$$\eta_v < \frac{2(\omega_{max} - 2\varepsilon_\theta)}{3v_{max}} \tag{13}$$

$$\Omega_{max} < \omega_{max} - \varepsilon_\theta \tag{14}$$

Further, $|\hat{\dot{\theta}}_d|$ is bounded $\forall\ t \geq 0$ thereby adhering to actuation limits of the robot.

Proof: With linear and angular velocity (v, ω) as the control input in kinematic model (2) of differential drive robot, we write the error dynamics as follows

$$\begin{aligned}
\dot{e}_x &= v\cos(\theta) - \dot{x}_d \\
&= v(\cos(e_\theta)\cos(\theta_d) - \sin(e_\theta)\sin(\theta_d)) - \dot{x}_d \\
\dot{e}_y &= v\sin(\theta) - \dot{y}_d \\
&= v(\sin(e_\theta)cos(\theta_d) + \cos(e_\theta)\sin(\theta_d)) - \dot{y}_d \\
\dot{e}_\theta &= \omega - \dot{\theta}_d
\end{aligned} \tag{15}$$

Using the expressions $\cos(\theta_d) = \frac{e_x}{D}$ and $\sin(\theta_d) = \frac{e_y}{D}$ and applying the controller (11)-(12) we obtain

$$\begin{aligned}
\dot{e}_x &= v_{max}\frac{\eta_v}{1+\eta_v D}(-e_x\cos^2(e_\theta) + e_y\cos(e_\theta)\sin(e_\theta)) - \dot{x}_d \\
\dot{e}_y &= v_{max}\frac{\eta_v}{1+\eta_v D}(-e_x\cos(e_\theta)\sin(e_\theta) - e_y\cos^2(e_\theta)) - \dot{y}_d \\
\dot{e}_\theta &= -(\omega_{max} - \Omega_{max})\tanh(\eta_v e_\theta) + \hat{\dot{\theta}}_d - \dot{\theta}_d
\end{aligned} \tag{16}$$

II-A. Lyapunov Analysis

We prove that the system (2) is ultimately bounded for the proposed controller (11), (12) using *Theorem 4.18* of [15]. In this analysis, we were able to construct Lyapunov candidate function separately for $D = \|e_x, e_y\|_2 = \sqrt{e_x^2 + e_y^2}$ & e_θ, and eventually established boundedness for the entire system. A small positive constant $0 < \zeta^3 \ll 1$ is chosen to define upper and lower bounds for the Lyapunov functions chosen for $D,\ e_\theta$, see (17), (23).

For Lyapunov analysis of $D = \sqrt{e_x^2 + e_y^2}$, we choose the Lyapunov candidate function $V_D : [0,\infty) \times \mathbb{R}^2 \to \mathbb{R}$ as follows

$$0 < \alpha_1(D) = \frac{D^2}{2+\zeta} \leq V_D(D) = \frac{D^2}{2} \leq \alpha_2(D) = \frac{D^2}{2-\zeta} \tag{17}$$

Here $\alpha_1,\ \alpha_2,\ V_D$ are class κ_∞ function. Then, the derivative of V_D along the trajectories of the error dynamics is

$$\begin{aligned}
\dot{V}_D &= D\dot{D} = e_x\dot{e}_x + e_y\dot{e}_y \\
\dot{V}_D &= -v_{max}\frac{\eta_v}{1+\eta_v D}\cos^2(e_\theta)(e_x^2 + e_y^2) - \dot{x}_d e_x - \dot{y}_d e_y
\end{aligned} \tag{18}$$

We define instantaneous velocity of desired trajectory as $v_{traj} = \dot{x}_d\hat{i} + \dot{y}_d\hat{j}$, $|v_{traj}| = \sqrt{\dot{x}_d^2 + \dot{y}_d^2}$ ($\hat{i},\ \hat{j}$ represent unit vector along x and y direction). Let the line joining the current position of robot, $(x(t), y(t))$, and the current reference point, $(x_d(t), y_d(t))$, be called L. The component of v_{traj} along L is denoted by $v_{traj}^L = \dot{x}_d\cos(\theta_d) + \dot{y}_d\sin(\theta_d)$, and the perpendicular component $v_{traj}^{\perp L} = \dot{y}_d\cos(\theta_d) - \dot{x}_d\sin(\theta_d)$, see Fig.3. Multiplying v_{traj}^L, $v_{traj}^{\perp L}$ with D, we get $Dv_{traj}^L(t) = \dot{x}_d e_x + \dot{y}_d e_y$ and $Dv_{traj}^{\perp L}(t) = \dot{y}_d e_x - \dot{x}_d e_y$.

$$\dot{V}_D \leq -\left(\frac{v_{max}\delta_\theta^2\eta_v D}{1+\eta_v D} + v_{traj}^L\right)D \leq -\left(\frac{v_{max}\delta_\theta^2\eta_v D}{1+\eta_v D} - |v_{traj}^{sup}|\right)D \tag{19}$$

[2]Theoretical explanation for $\varepsilon_\theta = \Omega(\tau)$ in (8) is provided in section III.B of [17]. Refer it to understand the dependence of ε_θ on τ.

[3]Refer section III-C of [17] to understand the role of ζ in finding the ultimate bounds on $D,\ e_\theta$.

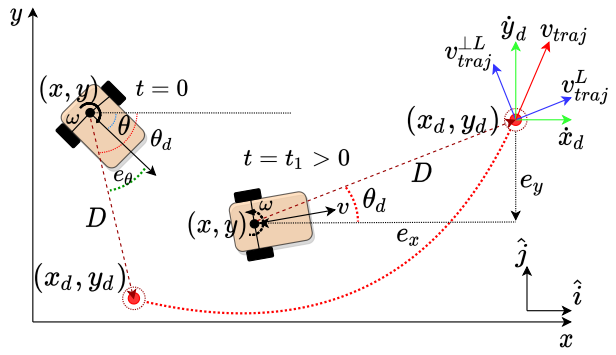

Fig. 3: Cartesian components of v_{traj} (Green): $(\dot{x_d},\dot{y_d})$, Components of v_{traj} along and $\perp$ to L (Blue): $(v^L_{traj},v^{\perp L}_{traj})$. D denotes the distance between $(x,\ y)$ and $(x_d,\ y_d)$

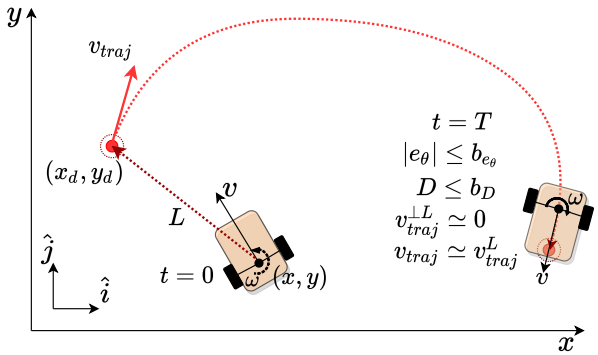

Fig. 4: Stable tracking achieved by differential drive robot using controller (11), (12)

$$\text{For } D\ge \mu_D=(1+\zeta)\frac{|v^{sup}_{traj}|}{\eta_v\left(v_{max}\delta^2_\theta-|v^{sup}_{traj}|\right)}>0$$

$$\dot{V}_D\le -\zeta|v^{sup}_{traj}|\left(\frac{v_{max}\delta^2_\theta-|v^{sup}_{traj}|}{v_{max}\delta^2_\theta+|v^{sup}_{traj}|}\right)D=-W(D)\le -W(\mu_D) \tag{20}$$

Note that $\alpha_1,\alpha_2,V_D\in\kappa_\infty$ class of functions and $W(D)$ is a continuous positive definite function. Hence, the result of *Theorem 4.18* of [15] will hold for any initial state $(e_x(0),\ e_y(0))$.

$$\begin{aligned}\left\|e_x,e_y\right\|_2=D(t)\le\alpha_1^{-1}(\alpha_2(\mu_D))\quad\forall\ t\ge T_D\\ D(t)\le\frac{\sqrt{2+\zeta}}{\sqrt{2-\zeta}}\mu_D=b_D\quad\forall\ t\ge T_D\end{aligned} \tag{21}$$

The value of T_D in (21) is determined as follows

$$\dot{V}_D\le -W(\mu_D)\implies\int_0^t\dot{V}_D\le\int_0^t-W(\mu_D)$$

$$V_D(t)-V_D(0)\le -W(\mu_D)t\implies V_D(t)\le V_D(0)-W(\mu_D)t$$

This shows that $V_D(D(t))$ reduces to $V_D(b_D)$ within the time interval of $[0,T_D]$ where,

$$T_D=\frac{V_D(D(0))-V_D(b_D)}{W(\mu_D)} \tag{22}$$

Unlike D, $e_\theta\in[-\cos^{-1}(\delta_\theta),\cos^{-1}(\delta_\theta)]\subseteq(-\pi/2,\pi/2)$. For e_θ, we choose the Lyapunov function candidate $V_{e_\theta}:[0,\infty)\times[-\cos^{-1}(\delta_\theta),\cos^{-1}(\delta_\theta)]\to\mathbb{R}$ as follows

$$0<\alpha_3(|e_\theta|)=\frac{e^2_\theta}{2+\zeta}\le V_{e_\theta}(|e_\theta|)=\frac{e^2_\theta}{2}\le\alpha_4(|e_\theta|)=\frac{e^2_\theta}{2-\zeta} \tag{23}$$

The derivative of V_{e_θ} along the trajectories of $e_\theta(t)$ is

$$\dot{V}_{e_\theta}=-(\omega_{max}-\Omega_{max})\tanh(\eta_\omega e_\theta)e_\theta+e_\theta(\dot{\hat{\theta}}_d-\dot{\theta}_d) \tag{24}$$

$$\dot{V}_{e_\theta}\le-\left((\omega_{max}-\Omega_{max})|\tanh(\eta_\omega e_\theta)|-\varepsilon_\theta\right)|e_\theta| \tag{25}$$

$$\text{For } |e_\theta|\ge\mu_{e_\theta}=\frac{(1+\zeta)}{2\eta_\omega}\ln\left(\frac{\omega_{max}-\Omega_{max}+\varepsilon_\theta}{\omega_{max}-\Omega_{max}-\varepsilon_\theta}\right)>0$$

$$\begin{aligned}\dot{V}_{e_\theta}\le-\left((\omega_{max}-\Omega_{max})\tanh(\eta_\omega\mu_\theta)-\varepsilon_\theta\right)|e_\theta|=-U(|e_\theta|)\\ \dot{V}_{e_\theta}\le-U(|e_\theta|)\le-U(\mu_{e_\theta})\end{aligned} \tag{26}$$

Note 4: μ_{e_θ} is strictly positive if $(\omega_{max}-\Omega_{max}-\varepsilon_\theta)>0$. Condition in (14) obtained.

V_{e_θ}, α_3, $\alpha_4\in\kappa$ class of functions and $U(|e_\theta|)$ is a continuous positive definite function in the domain of e_θ. To apply *Theorem 4.18* of [15] in this case, we choose $r=\cos^{-1}\delta_\theta-\zeta>0$. We find the value of $\alpha_4^{-1}(\alpha_3(r))=\sqrt{\frac{2-\zeta}{2+\zeta}}r$. Choosing sufficiently large positive value for η_ω will ensure $\mu_{e_\theta}<\alpha_4^{-1}(\alpha_3(r))$. By *Theorem 4.18* of [15], for every initial state $|e_\theta(0)|\le\alpha_4^{-1}(\alpha_3(r))\ \exists\ T_{e_\theta}\ge 0$ such that,

$$|e_\theta(t)|\le\alpha_3^{-1}(\alpha_4(\mu_{e_\theta}))=\frac{\sqrt{2+\zeta}}{\sqrt{2-\zeta}}\mu_{e_\theta}=b_{e_\theta}\ \forall\ t\ge T_{e_\theta} \tag{27}$$

$V_{e_\theta}(e_\theta(t))$ reduces to $V_{e_\theta}(b_{e_\theta})$ within the time interval 0f $[0,T_{e_\theta}]$ where, T_{e_θ} can be computed in the same way as T_D.

$$T_{e_\theta}=\frac{V_{e_\theta}(e_\theta(0))-V_{e_\theta}(b_{e_\theta})}{U(\mu_{e_\theta})} \tag{28}$$

By *Definition 4.6* of [15], $D(t)$ is globally uniformly ultimately bounded by b_D and $e_\theta(t)$ is uniformly ultimately bounded $b_{e_\theta}\ \forall\ t\ge T=\max\{T_D,T_{e_\theta}\}$.

II-B. Upper bound of $|\dot{\hat{\theta}}_d|$

We begin by obtaining an upper bound on $\dot{\theta}_d$ by starting with (6). Substituting (15), (16) in (6)

$$\begin{aligned}\left|\dot{\theta}_d\right|=\left|\frac{e_x\dot{e}_y-e_y\dot{e}_x}{D^2}\right|=\left|\frac{-Dv_{max}\sin(2e_\theta)\frac{\eta_v D}{2(1+\eta_v D)}-D(v^{\perp L}_{traj})}{D^2}\right|\\ \le\left|\frac{v_{max}\eta_v}{2(1+\eta_v D)}\right|+\frac{\left|v^{\perp L}_{traj}\right|}{D}\le\left|\frac{v_{max}\eta_v}{2(1+\eta_v D)}\right|+\frac{\left|v^{sup}_{traj}\right|}{D}\end{aligned} \tag{29}$$

In the region outside the ultimate bound: $D(t)\ge b_D$. Also,

$$b_D>\mu_D>\frac{|v^{sup}_{traj}|}{\eta_v\left(v_{max}\delta^2_\theta-|v^{sup}_{traj}|\right)}\ge\frac{|v^{sup}_{traj}|}{\eta_v\left(v_{max}-|v^{sup}_{traj}|\right)} \tag{30}$$

Therefore, by substituting the result of (30) and (29)

$$\begin{aligned}|\dot{\theta}_d|<\left|\frac{\eta_v(v_{max}-|v^{sup}_{traj}|)}{2}\right|+\eta_v(v_{max}-|v^{sup}_{traj}|)\\ |\dot{\theta}_d|<\frac{3\eta_v v_{max}}{2}\end{aligned} \tag{31}$$

Now, using (8) and upper bound on $|\dot{\theta}_d|$ in (31), we get

$$|\dot{\hat{\theta}}_d|\le|\dot{\theta}_d|+\varepsilon_\theta\implies|\dot{\hat{\theta}}_d|<\frac{3\eta_v v_{max}}{2}+\varepsilon_\theta \tag{32}$$

If we choose η_v as per (13), then choosing $\Omega_{max} = \frac{3\eta_v v_{max}}{2} + \varepsilon_\theta$ will satisfy (14). This way we have proved that $|\hat{\dot{\theta}}_d|$ is upper bounded for $D(t) \geq b_D$. Even if $D(t)$ goes arbitrarily close to zero, $|\hat{\dot{\theta}}_d|$ will remain upper bounded because

$$\lim_{D \to 0} \frac{|v_{traj}^{\perp L}|}{D} = 0 \tag{33}$$

A detailed proof of (33) is given in [17].

From the results of II-A, II-B, we conclude that stable tracking as defined in (10) is guaranteed without exceeding actuator limits.

II-C. Simulation Example

Example 1: To illustrate the results of Theorem 1, simulations were performed in MATLAB/Simulink. We applied the proposed controller in (11), (12) to an in-built Simulink model for differential-drive kinematics, see Fig.5. Time integration in the model was performed using ode45 solver with step size of $\tau = 0.01$ seconds.

In this example, initial pose of the robot is $[x(0), \ y(0), \ \theta(0)]^T = [0, \ -1, \ 0.5]^T$. Simulation time is set to $T_{sim} = 200$ seconds and the robot is required to track an elliptical trajectory $[x_d(t), y_d(t)] = \left[10\cos\left(\frac{2\pi t}{T_{sim}}\right), 6\sin\left(\frac{2\pi t}{T_{sim}}\right)\right]$ until the end of simulation time. Chosen control parameters are listed in Table I.

For $\zeta = 0.01$, we get $b_D = 0.163m$, and $b_{e_\theta} = 2.8 \times 10^{-3} rad$. It must be noted that the value of $b_D = 0.163m$ is 0.815% of the length of major axis of the elliptical trajectory. Higher peak angular speed of motors will yield even lower values of b_D, b_{e_θ}. The upper bound b_D on $D(t)$ can be reduced further by reducing the value of $|v_{traj}^{sup}|$.

Fig.6, Fig.7 shows the robot approaching the reference trajectory. The variation of control input $v(t), \omega(t)$ for $t \in [0, \ T_{sim}]$ is shown in Fig.8. It must be noted that $v(t)$, $\omega(t)$ does not exceed $v_{max} = 0.52\frac{m}{s}$, $\omega_{max} = 11.5\frac{rad}{s}$ respectively. Fig.9 highlights the convergence of D, $|e_\theta|$ to values within their respective ultimate bounds b_D, b_{e_θ}.

Controller parameters			
Parameter	Value	Parameter	Value
R	$0.02m$	η_v	10
L	$0.09m$	η_ω	10
$\omega_{r,\,l}^{max}$	$52^{rad}/_{s}$	τ	0.01
v_{max}	$0.52\ ^{m}/_{s}$	ε_θ	$0.1^{rad}/_{s}$
ω_{max}	$11.5^{rad}/_{s}$	Ω_{max}	$7.9^{rad}/_{s}$

TABLE I

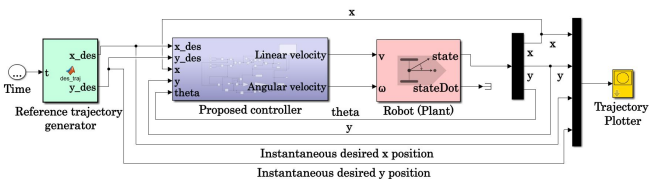

Fig. 5: Simulink model for trajectory tracking control of differential drive robot

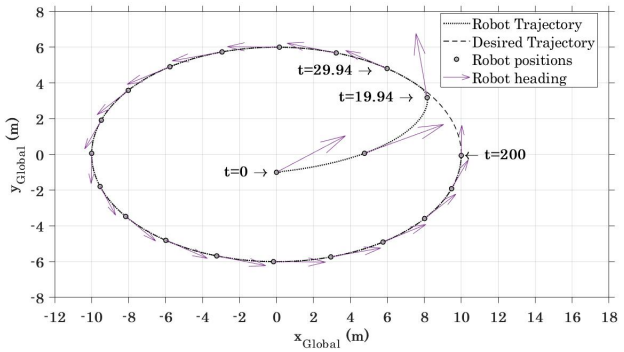

Fig. 6: Differential drive robot tracking elliptical trajectory using proposed controller (11), (12)

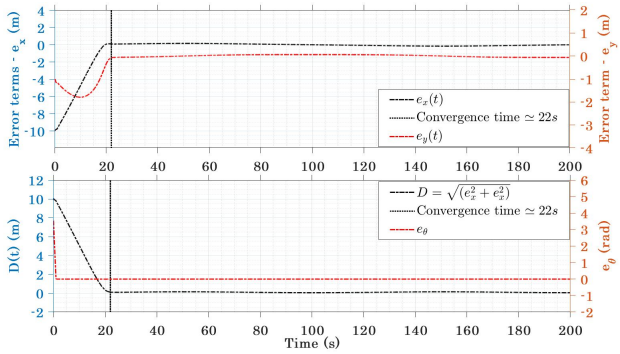

Fig. 7: Error terms - e_x, e_y, D, e_θ converging to neighbourhood around zero.

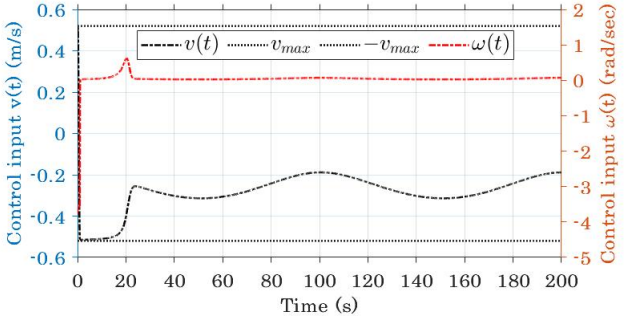

Fig. 8: Control inputs $v(t)$, $\omega(t)$ and their saturation limits

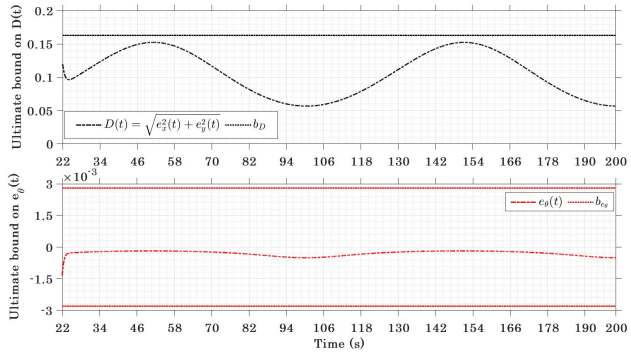

Fig. 9: $D(t)$, $e_\theta(t)$ ultimately bounded by b_D, b_{e_θ} respectively, for $t > 22s$

III. FORMATION CONTROL AND CONSTRAINT ON RADIUS OF FORMATION

In this section, we study the problem of formation control for a multi-robot system composed of N differential drive robots. The kinematic model of the robots with linear and angular velocity as control inputs, is described by

$$\begin{aligned} \dot{x}_i &= v_i \cos(\theta_i), \qquad x_i(0) = x_i^0 \\ \dot{y}_i &= v_i \sin(\theta_i), \qquad y_i(0) = y_i^0 \\ \dot{\theta}_i &= \omega_i, \qquad\quad \theta_i(0) = \theta_i^0 \end{aligned} \tag{34}$$

where $[x_i,\ y_i]^T \in \mathbb{R}^2$, $\theta_i \in \mathbb{R}$ and v_i, ω_i are linear and angular velocity of i^{th} robot respectively, where $i \in \{1,2,...N\}$.

We define the formation control problem as follows.

Problem 2: Given a desired formation for a group of N differential-drive robots and a reference trajectory, $[x_d(t),\ y_d(t)]$ for the center of formation. The objective for the robots is to converge to a stable formation around the center such that the center tracks the given desired trajectory while robots maintain the formation under set actuation limits. The controller must be implemented locally on each robot to achive the aforementioned task of formation control.

As mentioned in Section I, we address the formation control problem using the virtual-structure approach where we consider a virtual leader to generate the desired formation. We assign '0' as the index of the virtual leader. The desired position of follower robots is defined relative to the virtual leader using polar coordinates to create the desired formation shape, see Fig.10(a). It is possible to produce any formation shape by assigning appropriate polar coordinates to the follower robots.

We particularly consider circular formation and analyze the effects of its size on the kinematics of follower robots constituting the formation. We denote the formation radius by R_f. Each robot in the formation can access the instantaneous global pose of the virtual leader, $[x_0, y_0, \theta_0]^T$, see Fig.10(b).

At a particular instance of time, say $t \geq 0$, let $B_i^{des} = [x_i^{G.des}, y_i^{G.des}]^T$ be the desired global position of the i^{th} robot in the formation, and $b_i^{des} = [x_i^{l.des}, y_i^{l.des}]^T$ be its desired local position with respect to the coordinate system attached to the virtual leader $\forall\ i \in \{1,2,...,N\}$. The desired local position of the i^{th} robot (b_i^{des}) relative to virtual leader is defined using polar coordinates, (R_f, α_i), see Fig.10(a).

$$b_i^{des} = \begin{bmatrix} x_i^{l.des} \\ y_i^{l.des} \end{bmatrix} = \begin{bmatrix} R_f \cos(\alpha_i) \\ R_f \sin(\alpha_i) \end{bmatrix} \tag{35}$$

$$B_i^{des} = \begin{bmatrix} x_i^{G.des} \\ y_i^{G.des} \end{bmatrix} = \begin{bmatrix} x_0 \\ y_0 \end{bmatrix} + \begin{bmatrix} R_f \cos(\theta_0 + \alpha_i) \\ R_f \sin(\theta_0 + \alpha_i) \end{bmatrix} \tag{36}$$

Here, $[x_0,\ y_0] \in \mathbb{R}^2$ are the global coordinates of the virtual leader, and $\theta_0 \in \mathbb{R}$ is the orientation of virtual leader w.r.t the global x-axis. While defining the desired global position of followers in (36), the orientation of the virtual leader is taken into account to allow the entire formation to align itself with the orientation of the virtual leader, see Fig.10(a). Construction of circular formation using (35), (36) ensure that virtual leader will coincide with the center of formation

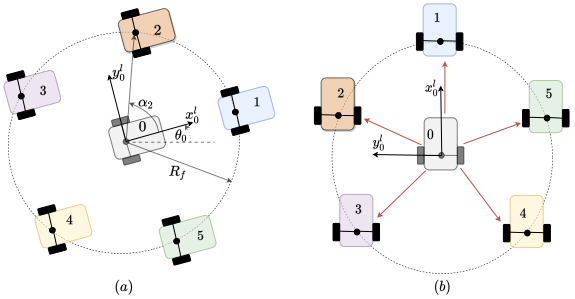

Fig. 10: (a) Circular arrangement of follower robots relative to virtual leader using polar coordinates $(R_f,\ \alpha_i)\ \forall\ i \in \{0,1,...,N\}$, (b) All followers receive instantaneous global pose of virtual leader, $[x_0,\ y_0,\ \theta_0]^T$

circle (not the centroid of robots' positions) after achieving the formation. Hence, we assign the reference trajectory, $[x_d(t),\ y_d(t)]$ to the virtual leader.

We aim to allow robots to converge to a stable circular formation such that the center of formation (coinciding with the virtual leader) tracks the given reference trajectory, $(x_d(t), y_d(t))$. This will be guaranteed if the error terms $e_{x_i}, e_{y_i}, e_{\theta_i}\ \forall\ i \in \{0,1,2,...,N\}$ converge to a neighbourhood close to the origin in finite time such that,

$$\begin{aligned} \sqrt{e_{x_i}(t)^2 + e_{y_i}(t)^2} = D_i(t) &\leq b_{D_i}\ \forall\ t \geq T_f \\ |e_{\theta_i}(t)| &\leq b_{e_{\theta_i}}\ \forall\ t \geq T_f \end{aligned} \tag{37}$$

for small positive numbers $b_{D_i}, b_{e_{\theta_i}} > 0\ \forall\ i \in \{0,1,2,...,N\}$.

Assumption 4: The formation radius R_f is strictly less than the minimum radius of curvature of the reference trajectory $[x_d(t),\ y_d(t)]$ for the center of formation circle, i.e.,

$$R_f < R_{des}^{min} = \underset{t>0}{\operatorname{argmin}} \left| \frac{(\dot{y}_d^2 + \dot{x}_d^2)^{1.5}}{\dot{x}_d \ddot{y}_d - \dot{y}_d \ddot{x}_d} \right| \tag{38}$$

and the choice of R_f as per (38) must also satisfy the following condition

$$|v_{traj}^{sup}| \left(1 + \frac{R_f}{R_{des}^{min}}\right) < v_{max} \tag{39}$$

where $|v_{traj}^{sup}| = \sup_{t \geq 0} \sqrt{\dot{x}_d^2 + \dot{y}_d^2}$.

Remark 3: Assumption 4 impose the following conditions on the soze of formation for a given reference trajectory.

1) Planned formation size must satisfy (38). If not, then the reference trajectory for robot closest to curvature center of $[x_d(t),\ y_d(t)]$ will not be smooth and will result in violation of assumption 1, leading to high angular velocities in robot (see Example 3 of III-B)
2) In addition to (38), the chosen value of R_f must also satisfy (39). The robot farthest from curvature center of $[x_d(t),\ y_d(t)]$ have to travel faster than other followers to keep the formation intact, hence condition in (39) must hold.
3) (38), (39) are essential for planning formations in a given scenario. These constraints are not explicit part of the controller but disobeying them will result in failure of formation due to above two listed reasons.

Manuscript 458 submitted to 2023 American Control Conference (ACC).
Received October 2, 2022.

4) Finding a similar condition for non-circular formation require a meticulous analysis of each robot's dynamics in formation. We will consider this in our future work.

Theorem 2. *Given a group of N differential drive robot whose kinematics are defined by (34). The maximum linear and angular speed of the robots are $v_{max}, \omega_{max} > 0$ respectively (3). Also, given a reference trajectory $[x_d(t),\ y_d(t)]$ for the formation center which satisfies assumptions $1-3$. The formation radius R_f is chosen such that (38), (39) holds. Then the robots will converge to a stable formation (37) around the virtual leader if the following controller is applied $\forall\ i \in \{0,1,2,...,N\}$*

$$v_i = -v_{max}\cos\left(e_{\theta_i}\right)\frac{\eta_v D_i}{1+\eta_v D_i} \tag{40}$$

$$\omega_i = -(\omega_{max}-\Omega_{max})\tanh\left(\eta_\omega e_{\theta_i}\right) + \hat{\theta}_{d_i} \tag{41}$$

for $D_i = \sqrt{e_{x_i}^2 + e_{y_i}^2}$ and positive constants $\eta_v,\ \eta_\omega,\ \Omega_{max} > 0$. The choice of η_v and Ω_{max} must satisfy (13), (14).

Proof: Consider the error dynamics of the robots in (15) $\forall\ i \in \{1,2,3...,N\}$. Using the expressions $\cos\left(\theta_{d_i}\right) = \frac{e_{x_i}}{D_i}$ and $\sin\left(\theta_{d_i}\right) = \frac{e_{y_i}}{D_i}$ and applying the controller (40), (41) to (15), we obtain the error dynamics in (16) $\forall\ i \in \{0,1,...,N\}$. As discussed previously, virtual leader is required to track the given reference trajectory $[x_d(t),\ y_d(t)]$.

III-A. Lyapunov Analysis

Similar to II-A, we pick separate Lyapunov functions to show the stability of D_i and e_{θ_i} $\forall\ i \in \{0,1,2,...,N\}$. We again choose ζ such that $0 < \zeta \ll 1$. For Lyapunov analysis of D_i $\forall\ i \in \{0,1,2,...,N\}$, we choose the function $V_D^f : [0,\infty) \times \mathbb{R}^{2(N+1)} \to \mathbb{R}$, and for e_{θ_i} $\forall\ i \in \{0,1,2,...,N\}$ we choose the Lyapunov candidate function $V_{e_\theta}^f : [0,\infty) \times (-\frac{\pi}{2}, \frac{\pi}{2})^{N+1} \to \mathbb{R}$.

$$V_D^f = \sum_{i=0}^{N}\frac{e_{x_i}^2 + e_{y_i}^2}{2} = \sum_{i=0}^{N}\frac{D_i^2}{2},\quad V_{e_\theta}^f = \sum_{i=0}^{N}\frac{e_{\theta_i}^2}{2} \tag{42}$$

Then we obtain the time derivatives of V_D^f and $V_{e_\theta}^f$ along the trajectories of error dynamics of all robots

$$\begin{aligned}\dot{V}_D^f &\le \sum_{i=0}^{N} -\left(\frac{v_{max}\delta_{\theta_i}^2\eta_v D_i}{1+\eta_v D_i} - |v_{traj}^{sup}|_i\right)D_i \\ \dot{V}_{e_\theta}^f &\le \sum_{i=0}^{N} -\left(\frac{(\omega_{max}-\Omega_{max})\eta_\omega|e_{\theta_i}|}{1+\eta_\omega|e_{\theta_i}|} - \varepsilon_\theta\right)|e_{\theta_i}|\end{aligned} \tag{43}$$

Similar to (20), (26), for $D_i(t) \ge \mu_{D_i}$ and $e_{\theta_i}(t) \ge \mu_{e_{\theta_i}}$ $\forall\ i \in \{0,1,...,N\}$ we get

$$\begin{aligned}\dot{V}_D^f &\le -W_i(D_i) \le -W_i(\mu_{D_i}) \\ \dot{V}_{e_\theta}^f &\le -U_i(e_{\theta_i}) \le -U_i(\mu_{e_{\theta_i}})\end{aligned} \tag{44}$$

where, $W_i(D_i), U_i(e_{\theta_i})$ are positive definite functions $\forall\ i \in \{0,1,...,N\}$. Choosing $\alpha_1^f, \alpha_2^f, \alpha_3^f, \alpha_4^f$ similar to (17), (23) such that $\alpha_1^f \le V_D^f \le \alpha_2^f$ and $\alpha_3^f \le V_{e_\theta}^f \le \alpha_4^f$, then the result of Theorem 1 can be applied to obtain ultimate bounds on D_i and e_{θ_i} $\forall\ i \in \{0,1,2,...,N\}$ as follows

$$\|e_{x_i}, e_{x_i}\|_2 = D_i(t) \le b_{D_i},\ |e_{\theta_i}(t)| \le b_{e_{\theta_i}}\ \forall\ t \ge T_f \tag{45}$$

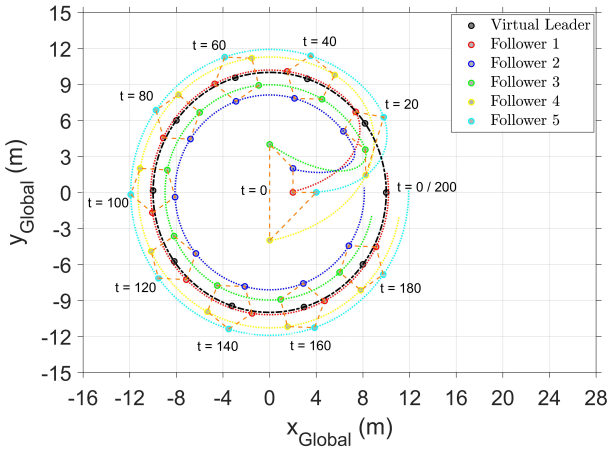

Fig. 11: Regular pentagonal formation ($R_f = 2$) of five differential-drive robots around the virtual leader

for small positive numbers $b_{D_i}, b_{e_{\theta_i}} > 0\ \forall\ i \in \{0,1,2,...,N\}$. Here, $T_f = \max_{i\in\{0,1,2,...,N\}}\{T_{D_i}, T_{e_{\theta_i}}\}$.

In II-B, note that Ω_{max} in (32) and upper limit on η_v in (13) are dependent only on v_{max}, ω_{max}. They can be applied directly for control of any formation along any desired trajectory. Hence, we conclude that robots will converge to stable formation around the virtual leader, and the formation center (which coincides with the virtual leader after stable formation is achieved) will track the given reference trajectory while robots keeping the formation intact under set actuation limits.

III-B. Simulation Examples

Example 2: To illustrate the results of Theorem 2 simulations were performed in MATLAB/Simulink. We implemented the proposed controller in (40), (41) to a group a $N = 5$ differential drive robots in Simulink environment. The virtual leader is also modelled using differential drive kinematics model in Simulink. For all robots, $v_{max} = 0.52^m/_s$. The robots have to converge to a regular pentagon like formation circumscribed by a circle of radius $R_f = 2m$ with virtual leader at its center. By assumption 4, we choose $R_{min}^{des} = 10m$ and $|v_{traj}^{sup}| = \frac{\pi}{10}^m/_s$. Rest of the control parameters are same as given in Table I. Based on the chosen values, the virtual leader is assigned a reference trajectory given by $[x_d(t), y_d(t)] = [10\cos(2\pi t/T_{sim}), 10\sin(2\pi t/T_{sim})]$, where T_{sim} is simulation time set to 200 seconds. The initial pose of virtual leader $[x_0^0,\ y_0^0,\ \theta_0^0] = [x_d(0),\ y_d(0), 1.57]$. The initial poses and local angular positions of the robots are given below.

$$\begin{bmatrix} x_1^0 & x_2^0 & x_3^0 & x_4^0 & x_5^0 \\ y_1^0 & y_2^0 & y_3^0 & y_4^0 & y_5^0 \\ \theta_1^0 & \theta_2^0 & \theta_3^0 & \theta_4^0 & \theta_5^0 \\ \alpha_1 & \alpha_2 & \alpha_3 & \alpha_4 & \alpha_5 \end{bmatrix} = \begin{bmatrix} 2 & 2 & 0 & 0 & 4 \\ 0 & 2 & 4 & -4 & 0 \\ 1 & -0.5 & 0 & -1 & 0 \\ 0 & 2\pi/5 & 4\pi/5 & 6\pi/5 & 8\pi/5 \end{bmatrix}$$

Results of example 2 are shown in Fig.11, which highlights a group of $N = 5$ robot converging to the desired formation around virtual leader, and the center of formation (coinciding with virtual leader) tracking the reference trajectory.

Example 3: In this example, we consider a circular formation of $N = 4$ robots with $R_f = 4m$.

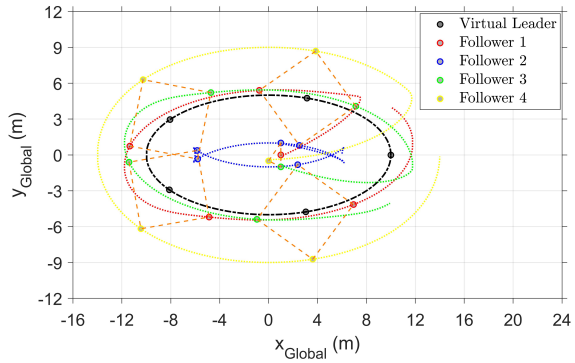

Fig. 12: Square formation ($R_f = 4m$) of four differential drive robots around the virtual leader

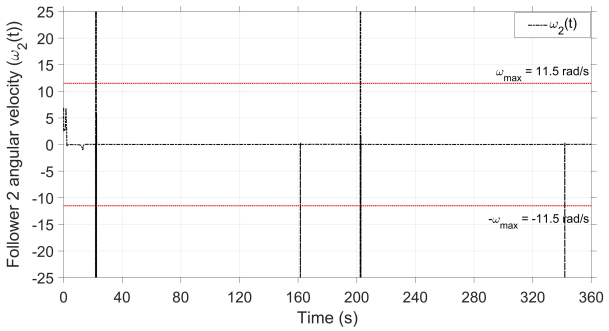

Fig. 13: Choice of $R_f = 4m > R_{min}^{des} = 2.5m$, violated assumption 4 resulting in $\omega(t) > \omega_{max}$ in Follower 2

The reference trajectory assigned to virtual leader is $[x_d(t), y_d(t)] = [10\cos(2\pi t/T_{sim}), 5\sin(2\pi t/T_{sim})]$, where $T_{sim} = 360s$. For the chosen reference trajectory, the value of $R_{des}^{min} = 2.5m$, $|v_{traj}^{sup}| = \pi/18 m/s$. Except $|v_{traj}^{sup}|$, control parameters listed in Table I are used. The initial pose of virtual leader $[x_0^0,\ y_0^0,\ \theta_0^0] = [x_d(0),\ y_d(0), 1.57]$. The initial poses and local angular position of robots for this example are as follows

$$\begin{bmatrix} x_1^0 & x_2^0 & x_3^0 & x_4^0 \\ y_1^0 & y_2^0 & y_3^0 & y_4^0 \\ \theta_1^0 & \theta_2^0 & \theta_3^0 & \theta_4^0 \\ \alpha_1 & \alpha_2 & \alpha_3 & \alpha_4 \end{bmatrix} = \begin{bmatrix} 1 & 1 & 1 & 0 \\ 0 & 1 & -1 & -0.5 \\ 1 & -1 & 0 & -1 \\ 0 & \pi/2 & \pi & 3\pi/2 \end{bmatrix}$$

Fig.12 displays the simulation results of example 3. We can observe a group of $N = 4$ robots in a square formation around the virtual leader tracking a elliptical trajectory. In Fig.12, the robot closest to the center of curvature of virtual leader's trajectory undergoes sharp turns at $[-10,\ 0]$, $[10,\ 0]$. Disobeying condition in (39) caused violation of assumption 1. Breach of angular velocity limits in Follower 2 can be observed in Fig.13.

IV. Conclusion and Acknowledgements

In this work, we have presented a novel control law for the circular formation of robots to track the desired trajectory. In particular, we guarantee boundedness to small errors under input saturation using Lyapunov analysis. We have further provided constraints on the formation size to prevent the violation of nonholonomic constraint and input limits. We believe practical input constraints are the key enablers in using the proposed controllers in real deployments. However, additional work is necessary to ensure robust control under measurement, actuator, and plant uncertainties before considering practical deployments. We also plan to integrate control barrier functions [18] with the proposed strategy to prevent collisions of robots with stationary and moving objects. We will consider these topics in our future work.

The authors would like to thank ARTPARK, IISc for the financial support provided as a part of their Research Internship Programme.

References

[1] S. Mastellone, D. M. Stipanovic and M. W. Spong, "Remote Formation Control and Collision Avoidance for Multi-Agent Nonholonomic Systems," Proceedings 2007 IEEE International Conference on Robotics and Automation, 2007, pp. 1062-1067.

[2] C. B. Low, "A Flexible Leader-Follower Formation Tracking Control Design for Nonholonomic Tracked Mobile Robots with Low-Level Velocities Control Systems," 2015 IEEE 18^{th} International Conference on Intelligent Transportation Systems, 2015, pp. 2424-2431.

[3] Luca Consolini, Fabio Morbidi, Domenico Prattichizzo, Mario Tosques, "Leader–follower formation control of nonholonomic mobile robots with input constraints," Automatica, Volume 44, Issue 5, 2008, Pages 1343-1349.

[4] S. Xiao, L. Feng, H. Lian and B. Du, "Dynamic formation and obstacle avoidance control for multi robot system," 2016 12^{th} World Congress on Intelligent Control and Automation (WCICA), 2016, pp. 59-63.

[5] C. M. Elias, S. K. El-Baklish, N. N. El-Ghandoor, O. M. Shehata and E. I. Morgan, "Practical Hybrid Graph-Based Formation Control Architecture for Leader-Follower Trajectory Tracking Problem," 2018 IEEE International Conference on Vehicular Electronics and Safety (ICVES), 2018, pp. 1-6.

[6] L. Yan and B. Ma, "Practical Formation Tracking Control of Multiple Unicycle Robots," in IEEE Access, vol. 7, pp. 113417-113426, 2019.

[7] D. Kostić, S. Adinandra, J. Caarls, N. van de Wouw and H. Nijmeijer, "Saturated control of time-varying formations and trajectory tracking-for unicycle multi-agent system," 49th IEEE Conference on Decision and Control (CDC), 2010, pp. 4054-4059.

[8] H. Liang, C. Wang, H. Chen and X. Wu, "A synchronous approach to trajectory tracking in multirobot formation control with time delays," 2013 IEEE International Conference on Information and Automation (ICIA), 2013, pp. 671-676.

[9] R. Dongxu and Y. Shuanghe, "Trajectory tracking control of circular formation of agents with tracking different reference variables," 2015 34th Chinese Control Conference (CCC), 2015, pp. 7563-7568.

[10] Wei Ren, Nathan Sorensen, "Distributed coordination architecture for multi-robot formation control". Robotics and Autonomous Systems, Volume 56, Issue 4, 2008, pp. 324-333.

[11] W. Dong and J. A. Farrell, "Cooperative Control of Multiple Nonholonomic Mobile Agents," in IEEE Transactions on Automatic Control, vol. 53, no. 6, pp. 1434-1448, July 2008.

[12] K. Cao, Gao Xiang and Hongyong Yang, "Formation control of multiple nonholonomic mobile robots," International Conference on Information Science and Technology, 2011, pp. 1038-1042.

[13] T. Balch and R. C. Arkin, "Behavior-based formation control for multirobot teams," in IEEE Transactions on Robotics and Automation, vol. 14, no. 6, pp. 926-939, Dec. 1998.

[14] M. Zhang, Y. Shen, Q. Wang and Y. Wang, "Dynamic artificial potential field based multi-robot formation control," 2010 IEEE Instrumentation & Measurement Technology Conference Proceedings, 2010, pp. 1530-1534.

[15] Hassan K. Khalil, 2002, *Nonlinear Systems*, Prentice Hall, 3*rd* ed.

[16] Unwrap function, MATLAB Version (R2020a), The MathWorks, Inc., Natick, Massachusetts, United States.

[17] Supplementary material. Ayush A., Mukunda B., Shishir K., "Formation control of differential-drive robots with input saturation and constraint on turning radius", 2022.

[18] A. D. Ames, S. Coogan, M. Egerstedt, G. Notomista, K. Sreenath and P. Tabuada, "Control Barrier Functions: Theory and Applications," 2019 18th European Control Conference (ECC), 2019, pp. 3420-3431.